Visible tomography of coherent modes in a linear magnetized plasma

P.A.S. David[1], A. Escarguel[1], Y. Camenen[1], J-P. Boeuf[2]

[1] *PIIM - UMR 7345 CNRS, Aix-Marseille Université, Marseille, France*

[2] *Université de Toulouse UPS, INPT / CNRS - LAPLACE, Toulouse, France*

Introduction

In this work, we study low frequency instabilities regularly, called 'flute modes', rotating around thie axis of the linear magnetized plasma device MISTRAL [1], [2] (see Fig.1). Different diagnostics have been used to study them, such as a fast camera, Langmuir probes, and laser induced spectroscopy. They have shown that those instabilities are driven by the local electric field creating an $\overrightarrow{E} \times \overrightarrow{B}$ drift, but there might also be a ionization front due to the azimuthal propagation of a shock wave [3], [4]. A simple analytical model has also been developed to study the physical parameters that control the plasma rotating frequency[5]. However, the physics of the instability is not yet completely understood.

We will use a newly implemented tomographic diagnostic, giving a spatial resolution without intrusion, to complement previous measurements. Then results from PIC simulations with parameters very close to the experiment will be shown.

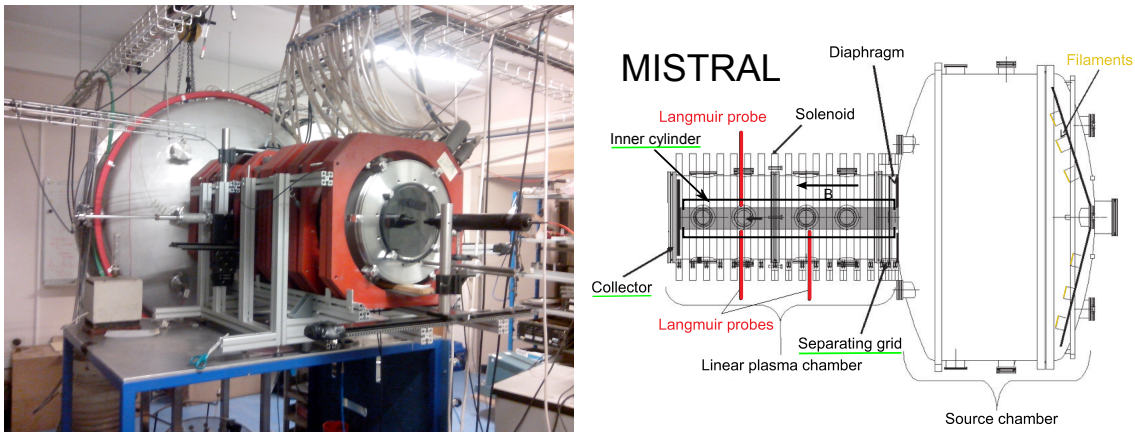

Figure 1 – MISTRAL device - Items underlined in green can be individually polarized to extract or to further confine electrons or ions in both longitudinal and radial direction.

Tomography diagnostic

In MISTRAL, the plasma is created in a large source chamber (1.4 m diameter, 1 m length) using a thermoionic discharge with 32 tungsten filaments and is then injected in a one meter long cylindrical magnetized interaction chamber. The plasma's behaviour is affected by several tunable parameters, such as the gas pressure ($1 - 6.10^{-4}$ mbar), the discharge energy ($30 - 40$ eV),

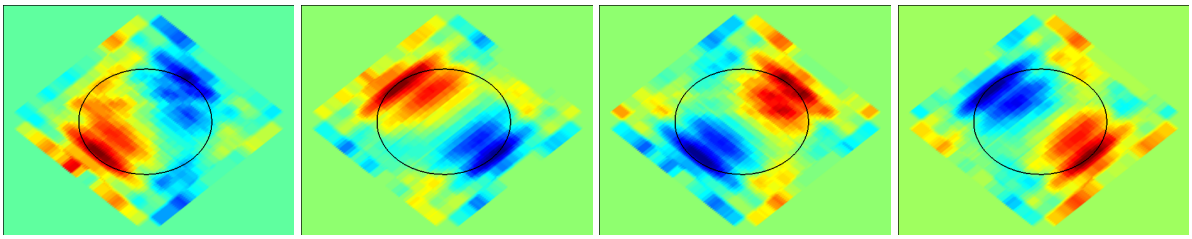

Figure 2 – Normalized emissivity pertubation ($\sim \widetilde{n}_e$) every 38.4 µs given by multiple-tomographic inversion on different pixels distributions (12x12 to 15x15 squares) for each experimental data. The black circle represent the position of the diaphragm.

the magnetic field intensity (150 Gauss), and the polarization of each end of the column (referred to as *separating grid* and *collector* in Fig.1) and of the inner cylinder (-25 to $+25$ V). The given windows of parameters are the one chosen to get stable modes rotating at 3 to 8 kHz.

We take advantage of the stability of those modes during several hours to simulates 32 simultaneous acquisitions using an optical single fibre moved to different positions and synchronizing the acquisitions with the plasma rotation. The fibre is collimated to collect light from a plasma cone between 8 and 13mm wide. A carbon based coating has been applied inside the vessel to limit excessive noise due to light reflections. Depending on the brightness of the plasma, two optical detectors can be used: a photomultiplier with a gain of about 10^{6-7}, or a photodiode. Both detectors measure the visible light from the plasma without spectral filtering. The light mainly comes from the argon lines, which in the coronal model, is directly proportional to the electron density n_e. Different tomographic inversions are made to compare the quality of each numerical method, and especially the pixels shapes.

The tomographic inversion diagnostic consists in measuring the plasma from n chords (collimated lines of sight), and using them to reconstruct the local plasma's emissivity. Here we use a finite-element technique [6] requiring to divide the cross-section of interest into m pixels then to calculate the contribution of each pixel to each detector to write the linear system $S = L.E$, S and E being the vectors of the n measurements, and of the m unknown emissivities respectively, and the n by m matrix $L = \left(l_{ij}\right)$, the volume of the i^{th} chord inside the j^{th} pixel. The main problems are that the matrix L is very ill conditioned, and that having a large number of pixels a limited number of measurements makes the system under-defined. So instead of directly solving this system, we look for E minimizing $\phi = \frac{1}{2}(L.E - S)^2 + \alpha\mathscr{R}$, with α a positive weighting parameter, and $\mathscr{R}$ a regularizing functional, here taken as the first order spatial derivative of the system [7]. No further hypothesis is made, for instance on the plasma shape or position.

Several parameters can cause numerical artefacts. The most important one is when measure-

ment chords and pixels positioning are almost aligned, for instance with parallel chords (e.g. vertical and horizontal) and a grid of square pixels. This is due to the first order differential regularization that causes the numeric signal to be spread along the direction of the spatial derivative, which is amplified by the geometry of both the pixels and the chords. On the other hand, such a regular grid has very simple and well defined finite differences, thus, improving the numerical calculations. To overcome this problem the mesh grid is rotated so that the pixels' sides and distribution are not parallel to the measurements. Remaining artefacts being much less important and more random, they can be further mitigated by doing several inversions on the same experimental data, but with different numerical pixels configurations (pixels numbers and rotation angle). The fig. 2 shows the time evolution of the emissivity perturbation obtained from tomographic inversions on different rotated 12x12, 13x13, 14x14 and 15x15 square grids from which the time averaged emissivity over several rotations is subtracted and no spatial smoothing was used. The frequency of the rotation from the tomography (one full rotation in $\sim (4 \times 38.4\ \mu\text{s})^{-1} \simeq 6.5$ kHz) corresponds to the frequency measured with a Langmuir probe. Additionally, we can see the density decreasing (blue region) on the opposite side of the expelled plasma arm (red region), which could not be measured with any other diagnostic and is consistent with numerical simulations showing the whole plasma center being dragged toward the instability.

Similar tests have been made with other configurations (up to seven time as many pixels as chords, different pixel shapes, other regularizing conditions) and can give similar results, but the previously described grid have given the most consistent ones. Finally, this study based on a single line of sight have been used to design a high resolution diagnostic to be installed during summer 2015 with a total of 128 lines of sight. The new set-up will first be tested and validated on global modes and then be used to study local turbulent modes.

Numerical simulations

A circular cross section of a cylindrical magnetized plasma is simulated using a Particles-In-Cell Monte-Carlo-Collisions code developed at LAPLACE (Toulouse, France) [8]. The third dimension is solely used for the energetic electron injection and particles loss through the extremities of the column so only modes with axial symmetry can be described. Here, as in the experiments, the key parameter to generate rotation modes is to extract enough particles in the radial direction compared to the axial one, or similarly to have a better confinement in the axial direction. In those simulations, very close to the experiment, the time average over several rotations of the plasma shows that such a configuration creates a potential well at the edge of the

diaphragm region (see fig. 3) which will force the excessive electrons to be radially expelled through an instability instead of freely drifting to the walls. The rotation movement of this instability then comes from a $\overrightarrow{E} \times \overrightarrow{B}$ configuration. There are ongoing studies to see whether the potential well can be experimentally measured on MISTRAL even though this variation only represents less than 25% of the maximum potential.

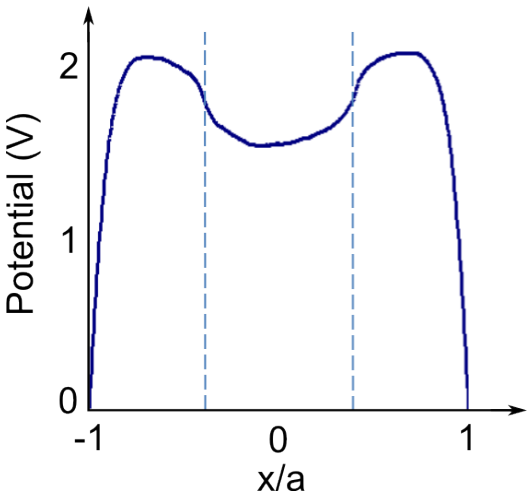

Figure 3 – Radial distribution of the potential in PIC simulations. The dashed lines represent the diaphragm diameter.

However, there is an important difference between simulations and the experiment in the axial direction. In the former there are two distinct regions at the end of the column, the negatively polarized separating grid in the middle, and the grounded diaphragm around it whereas in the latter the grid takes the whole diameter in front of the diaphragm which cannot be use to extract drifting particles. The axial confinement is therefore different. This difference is being studied and new simulations are running with a more adapted geometry trying to reproduce this behaviour.

This work has been carried out thanks to the support of the A∗MIDEX project (n○ ANR-11-IDEX-0001-02) funded by the "Investissements d'Avenir" French Government program, managed by the French National Research Agency (ANR)

References

[1] Th. Pierre, et al., Phys. Rev. Lett. **92**, 065004 (2004).
[2] A. Escarguel, Eur. Phys. J. D **56 (2)**, 209-214 (2010)
[3] S. Jaeger, et al., Phys. Plasmas **16**, 022304 (2009)
[4] C. Rebont, et al., Phys. Rev. Lett. **106(22)** (2011)
[5] B.M. Annaratone, Phys. Plasmas, **18 (3)** 032108 (2011)
[6] R.S. Granetz et P. Smeulders, Nuclear Fusion **28 (3)** (1988)
[7] M. Anton , et al., Plasma Physics and Controlled Fusion, **38 (11)**, 1849-1878 (1996)
[8] J.P. Boeuf et al., Phys. Rev. Lett. **111**, 155005 (2013)